



This is a repository copy of *Harvesting dissipated energy with a mesoscopic ratchet*.

White Rose Research Online URL for this paper:
<http://eprints.whiterose.ac.uk/87857/>

Version: Accepted Version

Article:

Roche, B., Roulleau, P., Jullien, T. et al. (4 more authors) (2015) Harvesting dissipated energy with a mesoscopic ratchet. *Nature Communications*, 6. 6738. ISSN 2041-1723

<https://doi.org/10.1038/ncomms7738>

Reuse

Unless indicated otherwise, fulltext items are protected by copyright with all rights reserved. The copyright exception in section 29 of the Copyright, Designs and Patents Act 1988 allows the making of a single copy solely for the purpose of non-commercial research or private study within the limits of fair dealing. The publisher or other rights-holder may allow further reproduction and re-use of this version - refer to the White Rose Research Online record for this item. Where records identify the publisher as the copyright holder, users can verify any specific terms of use on the publisher's website.

Takedown

If you consider content in White Rose Research Online to be in breach of UK law, please notify us by emailing eprints@whiterose.ac.uk including the URL of the record and the reason for the withdrawal request.



eprints@whiterose.ac.uk
<https://eprints.whiterose.ac.uk/>

Harvesting dissipated energy with a mesoscopic ratchet

B. Roche^{1,*}, P. Roulleau^{1,*†}, T. Jullien¹, Y. Jompol¹, I. Farrer², D.A. Ritchie², and D. C. Glattli¹

¹Nanoelectronics Group, Service de Physique de l'Etat Condensé, IRAMIS/DSM (CNRS URA 2464), CEA Saclay, F-91191 Gif-sur-Yvette, France

²Cavendish Laboratory, University of Cambridge, J.J. Thomson Avenue, Cambridge CB3 0HE, UK

* both authors contributed equally

The search for new efficient thermoelectric devices converting waste heat into electrical energy is of major importance. The physics of mesoscopic electronic transport offers the possibility to develop a new generation of nano-engines with high efficiency [1, 2, 3, 4]. Here we describe an all electrical heat engine harvesting and converting dissipated power into an electrical current. Based on a proposal by Büttiker and co-workers [5], two capacitively coupled mesoscopic conductors realized in a two-dimensional conductor form the hot source and the cold converter. In the former, controlled Joule heating generated by a voltage biased Quantum Point Contact results in thermal voltage fluctuations. By capacitive coupling the latter creates energy potential fluctuations in a cold chaotic cavity connected to external leads by two QPCs. For unequal QPC transmissions, a net electrical current is observed proportional to the heat produced. Compared with recent realizations based on spin [6, 7], superconductors [8, 9], and graphene [10] this mesoscopic ratchet device is simple and could be scaled for application in "molecular machinery" [11, 12, 13].

In his lectures [14], Feynman describes a ratchet coupled via an axle to a paddle wheel immersed in a fluid. Because of the Brownian motion of molecules, the paddle wheel has an equal probability to be rotated to the right or the left. The presence of the pawl preventing one rotation direction, say the left, the ratchet will rotate on the right, violating the second law of thermodynamics. The contradiction is solved and equal rotation probability restored by including thermal fluctuations of the pawl and ratchet. However if their temperature is smaller than that of the fluid, unidirectional rotation becomes possible, enabling conversion of heat into work. Figure 1(a) shows a SEM picture of our mesoscopic engine. It consists in two separate "cold" and "hot" circuit lines etched in a high mobility two-dimensional electron gas (2DEG) with two QPCs in each. Their temperature are T_2 and $T_1 > T_2$ respectively. The lower line is the heat source : the left QPC is tuned on a conductance plateau and DC biased in order to increase the temperature. The series QPC on the left is either tuned on a plateau or opened. To convert the heat into electrical current, it is necessary to define a mesoscopic ratchet together with its mesoscopic pawl. They are implemented in the upper cold circuit line. The ratchet is a chaotic electron cavity defined between two Quantum Point Contacts (QPCs) whose pawl is provided by breaking the symmetry of the energy dependent transmissions of the left and right QPCs. But, how to convert heat to DC current? A first step is the conversion of the thermal voltage fluctuations of the hot circuit into potential fluctuations of the cavity via the coupling capacitance C_C . Then, cold electrons entering the cavity can pick up some fluctuating energy $e\delta U$ before escaping into the external circuit via the QPCs,

see Fig.1(b). If the energy dependence of the transmission of the QPCs is different one can show that a unidirectional current occurs resulting from the detailed balance of electron flowing in and out the cavity by the left and right ports.

We now discuss how we proceed to heat the "hot" circuit and measure its temperature. We apply a DC bias V_{ds} across the left QPC while fixing its transmission D_h between 0 and 1. The series QPC is left opened. Joule heating with power $GV_{ds}^2/2$ is produced on both side of the QPC within a few electron-electron inelastic scattering lengths, $G = D_h 2e^2/h$ is the QPC conductance. A convenient way to measure the temperature T_e of electrons close to the QPC is to measure the low-frequency current noise. The power spectral density S_I is in general given by [15]:

$$S_I(V_{ds}) = 4k_B T_e G + 2FG(eV_{ds} \coth(\frac{eV_{ds}}{2k_B T_e}) - 2k_B T_e) \quad (1)$$

with k_B the Boltzmann constant, T_e the electronic temperature, G the conductance of the QPC, F the Fano factor defined as $F = \sum_n D_n(1 - D_n) / \sum_n D_n$ (D_n the transmission of the n th channel in the QPC) and $-e$ the charge of the electron. The noise contains information on the electron temperature and on the quantum partitioning of electrons by the QPC, the so-called shot noise. The partition statistics is characterized by the Fano factor which remarkably goes to zero when the QPC is tuned on a conductance plateau. Figure 2 shows the shot noise measurements as a function of V_{ds} for two different transmissions $D_1 = D_h = 0.2$ and 1, $D_{n>1} = 0$. On a conductance plateau the second term of Eq. 1, corresponding to shot-noise, is zero. The noise is only due to equilibrium thermal noise or Johnson Nyquist noise: $S_I(V_{ds}) = 4k_B T_e G$. Figure 2 for $D_h=1$ give a direct and accurate measurement of the electronic temperature as a function of applied bias. The increase of electronic temperature with Joule heating power is accurately described using the Wiedemann-Franz law of electron thermal conduction. This is fully applicable here as the gradient of electronic temperature, T_e from the QPC to base temperature at the Ohmic contacts, occurs on a length smaller than electron-phonon energy relaxation length. Combining the Joule power with the Wiedemann-Franz law, we expect [16, 17]:

$$T_W^2 = T_{fridge}^2 + \frac{24}{\pi^2} \frac{G}{G_m} (1 + \frac{2G}{G_m}) (\frac{eV_{ds}}{2k_B})^2 \quad (2)$$

with G_m the total conductance linking the QPC to the ohmic contacts, and T_{fridge} the base temperature. In Fig. 2, we have have plotted this law for $D_h \sim 1$ (black dashed line) and note a small disagreement with experimental data (blue dots). To circumvent this, we have to consider the cooling effect of the inner ohmic contact. We introduce the parameter α and write $T_e = T_W(1-\alpha) + \alpha T_{fridge}$. Setting $\alpha \sim 0.35$, we perfectly explain our measurements on the

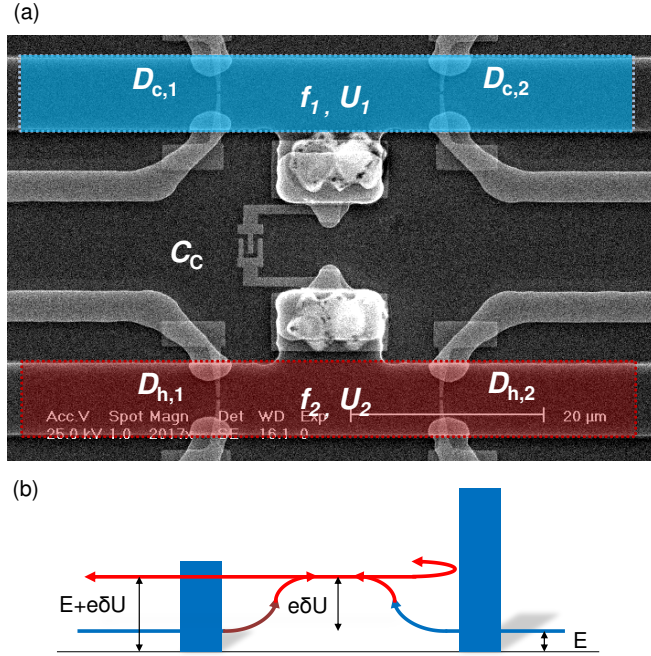


Figure 1: **a**, Scanning electron microscope view of the sample. Two lines defined by wet etching of the mesa are coupled via a coupling capacitance C_C . On the upper line (“cold” line) are patterned two QPCs in series that will define the chaotic cavity. On the lower line (“hot” line), a biased QPC enables to heat the line. The metallic capacitance is connected to the cavities via ohmic contacts visible on the picture. **b**, Schematic representation of the “cold” line. Once cold electrons enter the cavity, they experience voltage fluctuations and gain an energy $e\delta U$. Since QPC transmissions are tuned a two different transmissions a net current is generated.

plateau (blue solid line in Fig. 2). Once this temperature dependence is injected into (1), we also find an excellent agreement for $D_h = 0.2$ (red solid line in the Fig. 2). Typically, for an applied bias of 1 mV we get $\Delta T = T_2 - T_1 = 760$ mK.

We next investigate conversion of heat to current. A necessary condition to generate a net current is to create an asymmetry between the two QPCs of the cold circuit line. In a first experiment, we have tuned the second QPC at $D_{c,2} = 0.5$ and have swept the first QPC transmission $D_{c,1}$ between 0 and 2. To ensure the highest temperature difference ΔT between the two lines, both QPCs of the “hot” line are tuned on the first plateau (in fact the second QPC shows no good conductance plateau which may generate a small additional noise; this point will be discussed later). Then we increase by steps of ~ 1 mV the applied bias V_{ds} while sweeping the transmission. The difference traces of Fig. 3(a) show that the absolute value of the current increases with V_{ds} . It is zero when the transmission $D_{c,1} \sim$

0.5, i.e. when the detailed balance of input/output electrons is symmetrical. Then the current change sign as expected when the symmetry of the cavity is reversed, a hallmark of the ratchet effect. To model the current variation and have a quantitative understanding of the ratchet effect, we follow the semi-classical approach developed by Sothmann *et al.* [5]. Considering the symmetry-breaking in the energy-derivatives of the transmissions of the “cold” line, the authors find a DC current generated by heat conversion in the “cold” line given by:

$$I_c = \frac{\Lambda}{\tau_{RC}} k_B \Delta T \quad (3)$$

with Λ a rectification parameter, characterizing the asymmetry (the ratchet):

$$\Lambda = \frac{G'_{c,1} G_{c,2} - G'_{c,2} G_{c,1}}{G_{c,\Sigma}^2} \quad (4)$$

where $G_{c,i} = (e^2/h) D_{c,i}$, $G'_{c,i} = (e^3/h) D'_{c,i}$ (with $D'_{c,i} = \frac{\partial D_{c,i}}{\partial \epsilon}$) and $G_{c,\Sigma}$ the total conductance in parallel for the “cold” line.

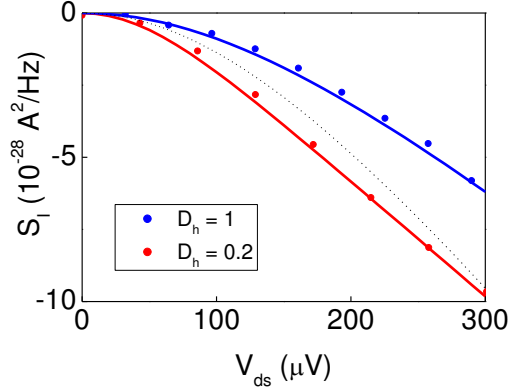


Figure 2: Current noise measurement as a function of the drain source bias for two different QPCs transmissions D_h of the “hot” line. The noise at $V_{ds} = 0$ as been subtracted. In blue $D_h = 1$, in red $D_h = 0.2$ (a feedback loop on the measured differential conductance ensures the stability of transmissions). At small bias, a QPC tuned on a plateau is noiseless. But at larger bias, the dissipated power combined with the Wiedemann-Franz law implies an elevation of the temperature and a larger Johnson Nyquist noise (black dotted line). The experimental values are perfectly accounted for when considering all three possible thermal anchors (blue solid line). For $D_h = 0.2$, we need to consider both usual shot noise together with this additional heating (red solid line).

We introduce G_{eff} an effective conductance of the double cavity, $G_{eff} = G_{c,\Sigma} G_{h,\Sigma} / (G_{c,\Sigma} + G_{h,\Sigma})$ ($G_{c,\Sigma} = G_{c,1} + G_{c,2}$, same for $G_{h,\Sigma}$) and C_{eff} ($C_{eff} = (C_\Sigma(2C_C + C_\Sigma)(C_\Sigma^2 + 2C_C C_\Sigma - C_C C_\mu) / 2C_C^2 C_\mu)$ with C_Σ the total capacitance of the lines and C_μ its total electrochemical capacitance [5]) which describes how strong the interaction is between the two cavities. $\tau_{RC} = \frac{C_{eff}}{G_{eff}}$ is an effective RC time of the double cavity.

In Fig. 3(a) we tune $D_{c,2} \sim 1$ and in Fig. 3(b) $D_{c,2} \sim 0.5$. In the first case, the derivative is zero and we should not have a change of the current sign (blue solid line in Fig. 3(b)) in agreement with our measurements. In the second one, the derivative of $D_{c,2}$ is non zero, and we expect a change of the current sign around $D_{c,1} \sim 0.5$ (blue solid line in Fig. 3(a)). In both cases, we check that by increasing the bias, we indeed enhance ΔT and measure a larger current.

We now discuss the measured current compared to the expected values. To obtain $G'_{c,i}$, one follows the saddle point model of a QPC [18] where the transmission of the n^{th} mode

can be written $D_{c,n}(V_g) = 1 / (1 + e^{2\pi(V_0 - V_g)/V_{g,n}})$ where $V_{g,n}$ is related to the negative curvature of the saddle point potential. The lever arm ($\Delta = \partial\epsilon / \partial V_g$) is extracted from transconductance ($dG_{c,i} / dV_g$) measurements $\Delta \sim 0.02e$. Since ΔT and G_{eff} are given, we extract $C_{eff} \sim 10\text{fF}$ in agreement with realistic values ([5]).

In this last part, we aim to proceed to a complete mapping of the current as a function of the two barriers of the cold line and to compare it with the theory. To do this, we apply a 2 mV DC bias on the hot line, we tune the first QPC on its first plateau while opening the second QPC (since the second QPC did not show well defined plateaus, by opening it we exclude any additional source of noise as partition noise; on the other hand it will strongly reduce the effective temperature difference). Measurements are plotted in Fig. 4(a). Since the second QPC of the hot line is opened, current fluctuations are reduced compared to the previous configuration and the current is smaller compared to Fig. 3(a). As expected, the current is zero

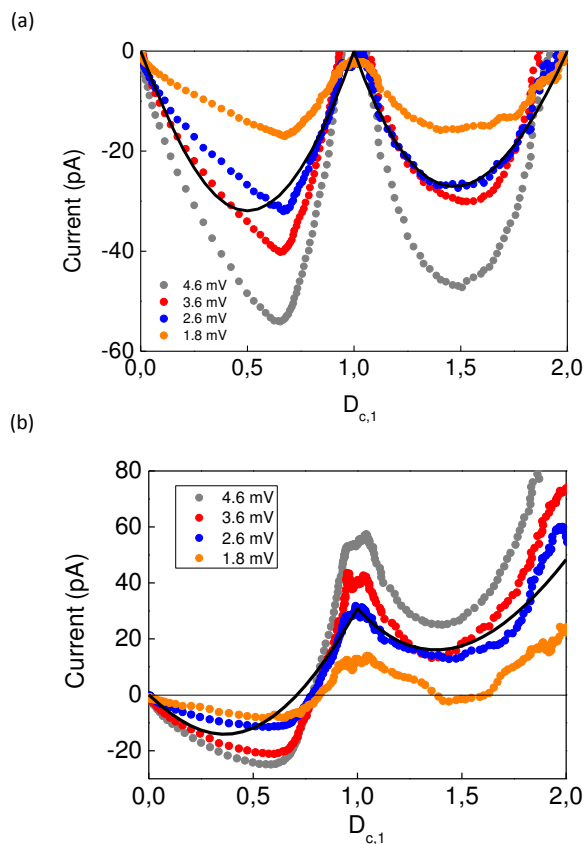


Figure 3: **a**, Current measured as a function of the first QPC transmission $D_{c,1}$ for $D_{c,2} = 1$. When temperature difference ΔT between the two lines is increased by applying a larger bias on the “hot” line, the current is enhanced. We sweep the applied bias from 1.8 mV to 4.6 mV. In solid line, theoretical prediction assuming $\Delta T_{eff} \sim 680\text{mK}$ **b**, Current measured as a function of the first QPC transmission $D_{c,1}$ for $D_{c,2} = 0.5$ for applied bias voltages from 1.8 mV to 4.6 mV. When $D_{c,1} \sim 0.5$, the symmetry of the cavity is reversed and the sign of the current changes. In solid line, theoretical prediction assuming $\Delta T_{eff} \sim 600\text{mK}$

when barriers transmissions are equal and maximum for the most asymmetric configuration. For example, for one of the two transmission tuned at 0.5 and the other one close to 1, the current is larger. We also check that the current changes of sign, when the role of the transmission is reversed. We compare these measurements with theoretical predictions in Fig. 4 (b). We observe an excellent quantitative behaviour with our data taking $C_{eff} \sim 200\text{fF}$, a reduction attributed to the opened series QPC in the hot line.

To summarize, we manage to realize a mesoscopic Brownian ratchet. A “hot” cavity is capacitively coupled to a “cold” mesoscopic ratchet composed of two QPCs in series. Depending on the symmetry of these two barriers, a current can be measured in the cold line. We have fully mapped the current as a function of these two barriers transmissions, in agreement with theoretical predictions. A considerable advantage of this system is the absence of direct electron thermal conduction as only capacitive coupling occurs. This is mandatory for good electrical energy harvesting. This set up is a proto-

type of a mesoscopic engine that would harvest dissipated energy transforming it into “ready-to-use” electrical current.

Methods

Emitter and detector lines were patterned using e-beam lithography on a high mobility two dimensional electron gas formed at the GaAs/Ga_{1-x}Al_xAs heterojunction. The two-dimensional electron gas 100 nm below the surface has a density of $1.8 \times 10^{11} \text{ cm}^{-2}$ and mobility $2.69 \times 10^6 \text{ cm}^2/\text{V s}$. Measurements were performed in cryogen free ³He cryostat with 300 mK base temperature. To elevate the electronic temperature of the hot line a finite V_{dc} is applied on the upper line. The resulting voltage fluctuations induce a photocurrent I_{ph} in the detector. We pulse V_{dc} at 1.5 kHz and detect the induced photocurrent using lock-in techniques.

Acknowledgement

The ERC Advanced Grant 228273 is acknowledged. The authors are grateful to P. Jacques for experimental support.

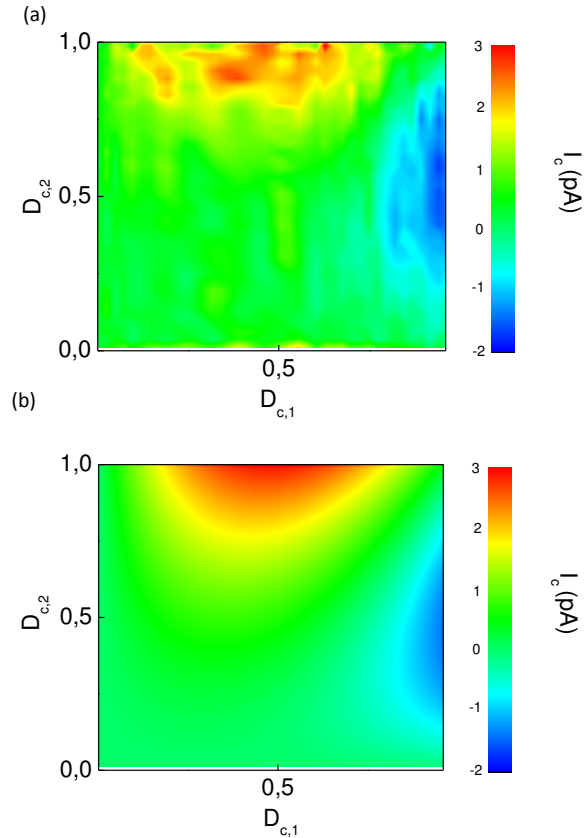


Figure 4: **a**, Color plot of the current measured in the cold line as a function of the first QPC transmission $D_{c,1}$ (x axis) and the second one $D_{c,2}$ (y axis). The applied bias on the hot line is equal to 2 mV. The first QPC of the “hot” line is tuned on the first plateau, although the series QPC is opened. When the symmetry of the barriers is inverted the sign of the current changes. **b**, Expected current as a function of both $D_{c,1}$ and $D_{c,2}$ for a $\Delta T \sim 50mK$. We recover experimental features, as a zero current along the line $D_{c,1}=D_{c,2}$, and a reverse current when the symmetry of the barriers is changed.

Author Contributions

D.C.G. designed the project. P.R., T.J., B.R. performed experiments, analysed data. P.R., D.C.G. wrote the manuscript Y.J. fabricated the sample. I.F. and D.A. Ritchie grew the wafer.

[†]Present address: Department of Physics, Mahidol University, Thailand

(†: preden.roulleau@cea.fr)

References

- [1] Giazotto, F., Heikkil, T., T., Luukanen, A., Savin, A., M. and Pekola J., P. , Opportunities for mesoscopics in thermometry and refrigeration: Physics and applications, *Rev. Mod. Phys.* **78**, 217 (2006)
- [2] Whitney, R., Thermodynamic and quantum bounds on nonlinear dc thermoelectric transport, *Phys. Rev. B* **87**, 115404 (2013)
- [3] Meair, J. and Jacquod P., Scattering theory of nonlinear thermoelectricity in quantum coherent conductors, *J. Phys.: Condens. Matter* **25** 082201 (2013)
- [4] López, R., and Sánchez, D. , Nonlinear heat transport in mesoscopic conductors: Rectification, Peltier effect, and Wiedemann-Franz law, *Phys. Rev. B* **88**, 045129
- [5] Sothmann, B., Sánchez, R., Jordan, A.N. and Büttiker, M. Rectification of thermal fluctuations in a chaotic cavity heat engine *Phys. Rev. B*, **85** 205301, 2012.
- [6] Costache, M.V. and Valenzuela, S.O. Experimental Spin Ratchet *Science*, **330** 1645, 2010.
- [7] Hwang, S.-Y., Lim, J., S. , López, R., Lee, M., and Sánchez D., Proposal for a local heating driven spin current generator, *Appl. Phys. Lett.* **103**, 172401 (2013)
- [8] Villegas, J.E. et al. A Superconducting Reversible Rectifier That Controls the Motion of Magnetic Flux Quanta *Science*, **302** 1188, 2003.

- [9] Togawa, Y. et al. Direct Observation of Rectified Motion of Vortices in a Niobium Superconductor *Phys. Rev. Lett.*, **95** 087002, 2005.
- [10] Drexler, C. et al. Magnetic quantum ratchet effect in graphene *Nat. Nanotechnology*, **8** 104, 2013.
- [11] Koumura, N., Zijlstra, R. W. J., van Delden, R.A., Harada, N. and Feringa, B.L. Light-driven unidirectional molecular, *Nature*, **401** 152, 1999.
- [12] Bermudez, V. et al., Influencing intramolecular motion with an alternating electric field, *Nature*, **406** 608, 2000.
- [13] Serreli, V., Lee, C.-F., Kay, E.R. and Leigh, D.A. A molecular information ratchet, *Nature*, **445** 523, 2007.
- [14] Feynman, R. P., Leighton, R., B., and Sands, M. *Lect. 1.46*, **1** 46, 1966.
- [15] Blanter Ya., M., and Büttiker, M., Shot Noise in Mesoscopic Conductors, *Phys. Rep.* **336**, 1 (2000)
- [16] Kumar, A., Saminadayar, L., Glattli, D.C., Jin, Y. and Etienne, B., Experimental Test of the Quantum Shot Noise Reduction Theory, *Phys. Rev. Lett.*, **76** 2778, 1996.
- [17] Steinbach, A.H., Martinis, J.M. and Devoret, M.H. Observation of Hot-Electron Shot Noise in a Metallic Resistor, *Phys. Rev. Lett.*, **76** 3806, 1996.
- [18] Büttiker, M., Quantized transmission of a saddle-point constriction, *Phys. Rev. B*, **41** 7906(R), 1990.